Chapter 2

Microwave Open Resonator Techniques - Part II: Applications

Sandra Costanzo, Giuseppe Di Massa and Hugo Oswaldo Moreno

Additional information is available at the end of the chapter

http://dx.doi.org/10.5772/50996

1. Introduction

The accurate modelling of dielectric and impedance features [1, 2] is an essential need for the efficient design of microstrip circuits and antennas. The increasing demand for miniaturization and high-frequency operation strongly imposes the accurate characterization of low-loss thin dielectric surfaces [12, 14], both in the form of simple laminated substrates [6, 9, 19, 23], as well as in more complex configurations of microstrip grids to be used for reflectarray/transmitarray structures [3, 21]. Various microwave techniques have been introduced in literature to characterize the electrical properties of materials. They include open-ended waveguide/coaxial probe methods [18], free-space techniques [16], stripline [20], transmission/reflection [4] and resonant [22] procedures, all having specific advantages and constraints. Among them, open resonator methods [10, 11, 13, 15, 17, 25] give the most powerful tool to accurately retrieve the equivalent impedance properties of low-loss thin dielectric surfaces. In the standard resonator approach [25], approximate empirical formulas are adopted to obtain the surface impedance characterization from the knowledge of measured resonance parameters, such as the frequency shift and the cavity quality factor. Information from different sample thicknesses and/or positioning are generally adopted to increase the accuracy in the surface parameters extraction, which is performed in terms of a transcendental equation having multiple roots [11].

All existing papers on open resonator methods inherit the approach proposed in [25], thus assuming an ideal open cavity and neglecting the excitation of higher-order modes, which have a great relevance for an accurate modelling of the coupling with the feeding waveguide. In this chapter, an equivalent circuit formulation is adopted to accurately model the open resonator behavior in the presence of the test surface. On the basis of a complete modal analysis as outlined in [5], the adopted circuit approach leads to optimize the coupling between the cavity and the exciting waveguide, further including a proper modelling of the cavity losses, which provides a significant improvement when compared to the traditional open resonator approach [25].

The chapter is organized as follows. In Section 2, a detailed description of the equivalent circuit formulation is provided and an accurate expression is derived for the equivalent impedance of the test planar surface. In Section 3, the adoption of the proposed approach for the dielectric characterization of thin grounded dielectric substrate is presented. A further application of the method to the phase response characterization of microstrip reflectarray elements is provided in Section 4. Conclusions are finally outlined in Section 5.

2. Equivalent circuit model of open resonator system for the characterization of planar surfaces

The open resonator system adopted for the equivalent impedance characterization is illustrated in Fig. 1. It consists of a spherical mirror of radius R_o, which is used to produce a Gaussian beam impinging on the grounded test surface at a distance l. A feeding rectangular waveguide of standard height b is adopted for the cavity excitation, and a transition giving a final height b_1 is properly designed to optimize the coupling with the cavity.

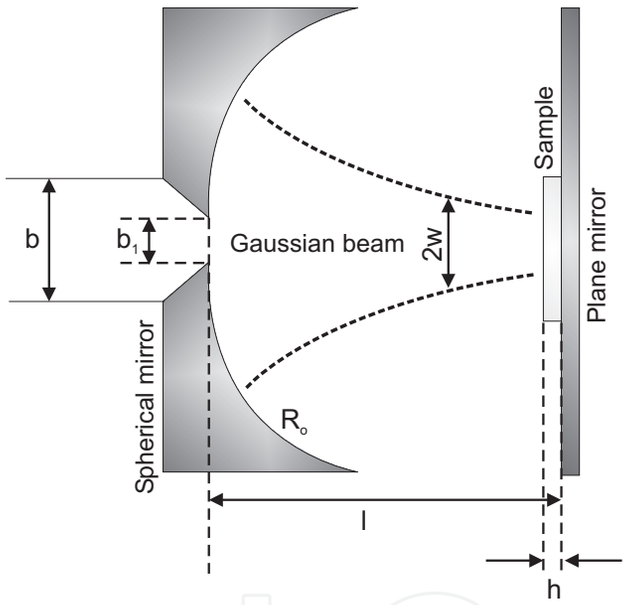

Figure 1. Hemispherical open resonator system

At this purpose, the approach proposed in [5] is adopted, which is based on a complete eigenfunctions analysis leading to the equivalent circuit of Fig. 2 [8].

The relative circuit parameters, accurately defined in [5] and reported in Table 1, properly take into account for the ohmic and the diffraction losses of the cavity. In particular, the component R' models the losses due to the finite conductivity of the mirrors, while the term L' gives the effect of the skin depth δ. It sums to the inductive circuit part L_o modelling the cavity, thus producing a shift in the resonant frequency, which is equivalent to a cavity enlargement.

In Table 1, the term $2l$ gives the cavity length, a is the major waveguide dimension, σ represents the conductivity, while $k_o = 2\pi f_o / c$ is the free-space propagation constant, c being the velocity of light and f_o the resonant frequency of the empty resonator.

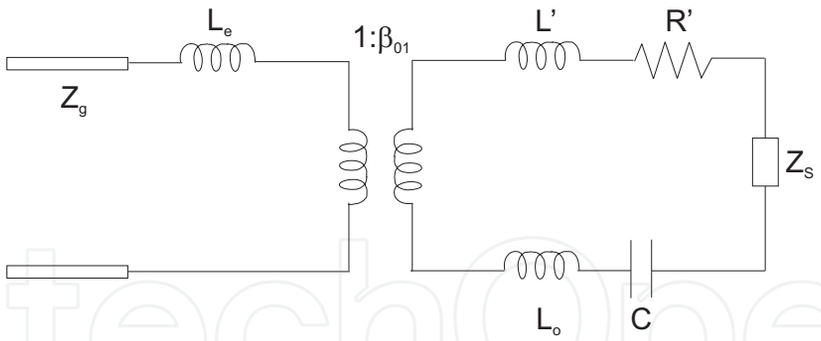

Figure 2. Equivalent circuit of open resonator system

L_o [H]	L' [H]	L_e [H]	C [F]	R' [Ω]
$\mu_o l$	$\mu_o \delta$	$16.5 \cdot 10^{-3} \mu_o a$	$\frac{\epsilon l}{(k_o l)^2}$	$\frac{2}{\sigma \delta}$

Table 1. Expressions of circuit parameters in Fig. 2

From the circuit reported in Fig. 2 it is easy to derive the expressions of the waveguide input impedance Z_i and the reflection coefficient Γ, respectively given as [8]:

$$Z_i = j\omega L_e + \frac{Z_R}{\beta_{01}^2} \tag{1}$$

$$\Gamma = \frac{Z_i - Z_g}{Zi + Z_g} \tag{2}$$

where:

$$Z_R = j\omega L_T + R' + \frac{1}{j\omega C} \tag{3}$$

$$L_T = L_o + L' \tag{4}$$

while β_{01} is the waveguide-cavity factor as reported in [5] and Z_g represents the characteristic impedance of the transmission line equivalent to the rectangular waveguide excited in its fundamental mode TE_{10}.

The insertion of the grounded test surface results into an equivalent impedance Z_S (Fig. 2), which can be easily expressed as [8]:

$$Z_S = jZ_d tan\left(k_d h - \phi_G\right) \tag{5}$$

The terms Z_d and k_d into eq. (5) respectively give the characteristic impedance and the propagation constant of the shorted transmission line equivalent to the grounded dielectric slab, while the phase shift ϕ_G takes into account for the Gaussian nature of the beam, and is given as [7]:

$$\phi_G = arctan\left(\frac{h}{d_R}\right) \tag{6}$$

where $d_R = \sqrt{Rl - l^2}$ is the Rayleigh distance.

Due to the negligible contribution of the Gaussian amplitude variation, a uniform wave is assumed, leading to use an equivalent circuit approach, while the phase term ϕ_G introduced by the Gaussian beam is properly considered to model the associated resonance frequency shift.

It is straightforward to deduce the equivalent impedance Z_S of eq. (5) from return loss measurements performed at the waveguide input, under empty and loaded cavity conditions. As a matter of fact, the insertion of the test surface sample produces a shift in the resonant frequency of the cavity, from which the imaginary part of impedance Z_S can be derived. At the same time, an amplitude reduction of the reflection coefficient is obtained in the presence of the grounded slab, which in turns is related to real part of impedance Z_S.

In the following Sections, a more detailed description of the impedance reconstruction method is provided for two specific application contexts, namely the complex permittivity retrieval of thin dielectric substrates and the phase response characterization of microstrip reflectarrays.

3. Open resonator application to dielectric material characterization

Let us consider as test surface a grounded dielectric sheet having thickness h (Fig. 1) and unknown complex permittivity $\epsilon = \epsilon' - j\epsilon''$. Under this hypothesis, the equivalent impedance Z_S can be easily expressed as [8]:

$$Z_S = j\frac{Z_o}{a_\epsilon\left(1 - jb_\epsilon\right)} tan\left\{k_o\left[a_\epsilon\left(1 - jb_\epsilon\right)\right]h - \phi_G\right\} \tag{7}$$

where $a_\epsilon = \sqrt{\epsilon'}$, $b_\epsilon = \frac{1}{2}tan\delta$, Z_o and k_o being, respectively, the free-space impedance and propagation constant.

After some manipulations, the real and imaginary parts of impedance Z_S can be derived as follows [8]:

$$Re\{Z_S\} = \frac{Z_o}{a_\epsilon\left(b_\epsilon^2 + 1\right)} \cdot \frac{sinh\left(2a_\epsilon b_\epsilon hk_o\right) - b_\epsilon sin\left\{2\left[a_\epsilon hk_o + arctan\left(\frac{\lambda h}{\pi w^2}\right)\right]\right\}}{cosh\left(2a_\epsilon b_\epsilon hk_o\right) + cos\left\{2\left[a_\epsilon hk_o + arctan\left(\frac{\lambda h}{\pi w^2}\right)\right]\right\}} \tag{8}$$

$$Im\{Z_S\} = \frac{Z_o}{a_\epsilon\left(b_\epsilon^2 + 1\right)} \cdot \frac{sin\left\{2\left[a_\epsilon hk_o + arctan\left(\frac{\lambda h}{\pi w^2}\right)\right]\right\} + b_\epsilon sinh\left(2a_\epsilon b_\epsilon hk_o\right)}{cosh\left(2a_\epsilon b_\epsilon hk_o\right) + cos\left\{2\left[a_\epsilon hk_o + arctan\left(\frac{\lambda h}{\pi w^2}\right)\right]\right\}} \tag{9}$$

They have two distinct effects on the resonance response at the waveguide input. The imaginary part $Im\{Z_S\}$ is responsible for a shift in the resonant frequency of the cavity, with respect to the empty case, while the real part $Re\{Z_S\}$ produces an amplitude reduction of the input reflection coefficient. The measurement of these two information can be, in principle, adopted to retrieve the unknown complex permittivity $\epsilon' - j\epsilon''$. However, due to the high quality factor Q of the cavity, which is equivalent to a very narrow resonant bandwidth, it is very difficult to measure the exact value of the reflection coefficient, and consequently the dielectric loss.

In alternative way, the information relative to the resonant frequencies of the empty and loaded cavity, respectively equal to f_o and f_L, can be used to retrieve the imaginary part $Im\{Z_S\}$. On the other hand, the real part $Re\{Z_S\}$ can be derived from the knowledge of the loaded dielectric quality factor Q_L, which is inversely proportional to the difference between the $3dB$ frequencies at each side of the resonance minimum. Finally, from the conjuncted knowledge of the two left terms of eqs. (8) and (9), the terms a_ϵ and b_ϵ can be retrieved, which are related to the real and imaginary parts of the unknown complex permittivity of the test surface.

The numerical implementation of the above dielectric characterization method is performed by a two step procedure, summarized as follows:

1. the imaginary part ϵ'' is first neglected and eq. (9) is solved with respect to the variable a_ϵ, directly related to the real part ϵ';
2. the value computed into step 1 is inserted into eq. (8) to retrieve the term b_ϵ, which in turns is related to the dielectric loss tangent, and thus to the imaginary part ϵ''.

3.1. K-band dielectric characterization of thin dielectric substrates

The equivalent circuit approach for the complex permittivity retrieval of planar surfaces is applied to accurately design a K-band open resonator system fed by a standard WR62 rectangular waveguide. As a primary task, the waveguide-to-cavity transition is accurately dimensioned to optimize the coupling and thus the efficiency of the open resonator system. At this purpose, the equivalent circuit approach proposed in [5] is adopted to perform a parametric analysis of the reflection coefficient at the waveguide input as a function of the waveguide height b (Fig. 3) for a fixed design frequency f_o = 24 GHz.

Due to the mechanical tolerances of the available machine, a value b_1 = 0.7 mm (Fig. 1), slightly larger than that giving the minimum reflection coefficient, is adopted for the smaller height of the transition, starting from the standard WR62 value b =4.3 mm.

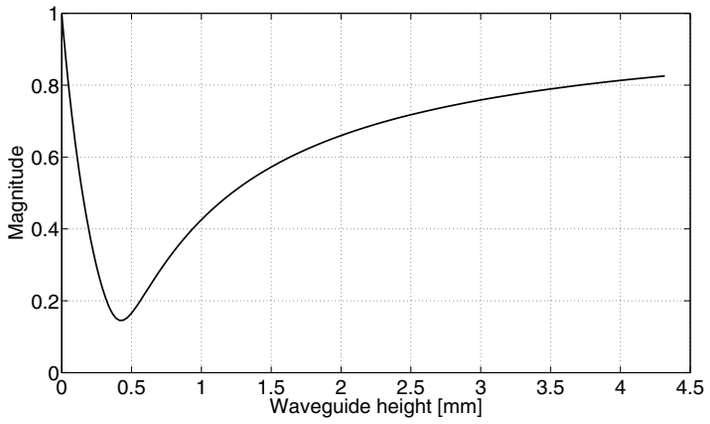

Figure 3. Reflection coefficient at the waveguide input vs. waveguide height b

The open resonator is realized on Aluminum material, by assuming a radius R_o = 517 mm and a distance l = 490 mm between the mirrors, this latter giving the excitation of a $TEM_{0,0,76}$

mode inside the cavity. The open resonator radius, the longitudinal mode number and the relative length l are derived by a compromise choice on the basis of the following parameters:

- the fixed design frequency;
- the resonator stability;
- a proper waist on the mirror to avoid diffraction losses;
- a waist value on the sample greater than a wavelength in order to measure the diffraction features of the resonant structures.

A photograph of the realized K-band open resonator system, connected to a Vector Network Analyzer, is illustrated in Fig. 4.

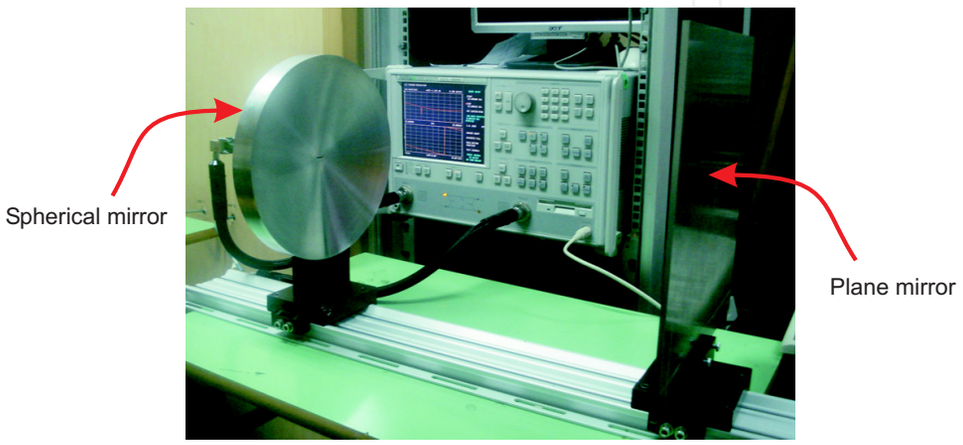

Figure 4. Photograph of realized K-band open resonator system

In order to test the proposed dielectric characterization technique, three standard substrates usually adopted for the realization of microwave planar structures are considered as test surfaces. The materials names and their nominal parameters as available from the producer are reported in Table 2.

Index	Material	Thickness h [mm]	ϵ' @ 10 GHz	tan δ @ 10 GHz
1	Arlon AR600	0.762	6	0.0030
2	Arlon DiClad 527	0.762	2.55	0.0018
3	Arlon 25FR	0.762	3.58	0.0035

Table 2. Nominal parameters of test dielectric substrates

The measured return loss under empty and loaded cavity conditions are reported in Figs. 5-7. As expected from the theory outlined in the previous Section, a frequency shift and an amplitude reduction can be observed for all tested dielectrics after the introduction of the samples.

In order to retrieve the unknown complex permittivity of the substrates under test, the frequency shift $\Delta f = f_o - f_L$ is measured together with the 3 dB frequencies f_1, f_2 at each side of the resonant frequency f_L. These quantities, together with the loaded quality factor Q_L and the values of ϵ' and tan δ, as retrieved from eqs. (8)-(9) are reported in Table 3. An excellent agreement with the nominal parameters reported in Table 2 can be observed.

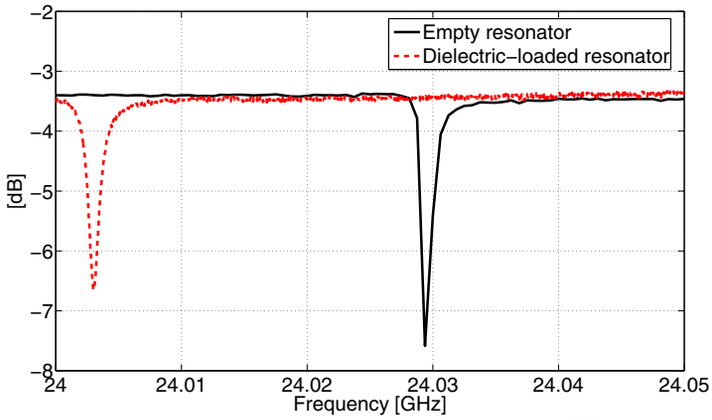

Figure 5. Measured return loss for test material 1: comparison between empty and loaded cavity conditions

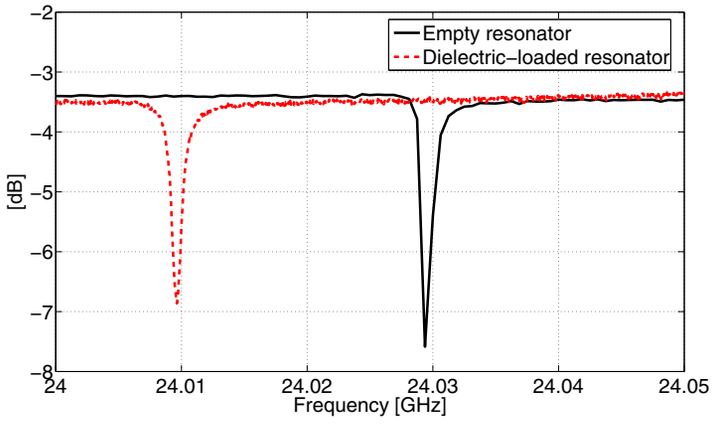

Figure 6. Measured return loss for test material 2: comparison between empty and loaded cavity conditions

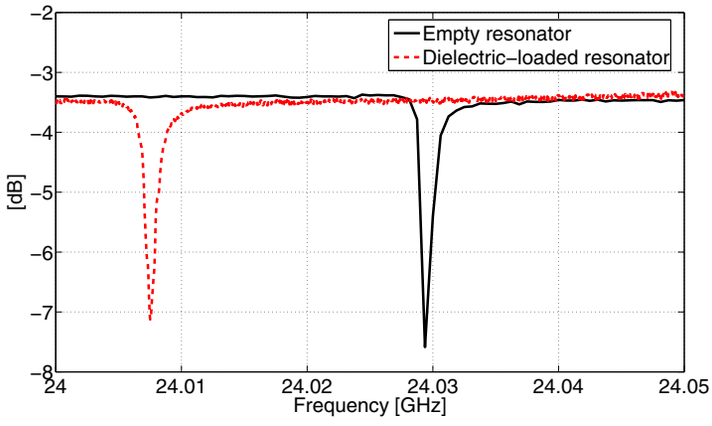

Figure 7. Measured return loss for test material 3: comparison between empty and loaded cavity conditions

Material Index	f_L [GHz]	f_1 [GHz]	f_2 [GHz]	Δf [MHz]	Q_L	ϵ'	tan δ
1	24.003	24.0018	24.0045	2.7	8890	6	0.00324
2	24.00965	24.00918	24.00995	0.77	31181	2.535	0.002
3	24.00752	24.00698	24.0084	1.42	16907	3.54	0.004

Table 3. Measured parameters and retrieved complex permittivity of test dielectric substrates

4. Open resonator application to microstrip reflectarray elements characterization

Synthesis procedures for the reflectarrays design [24] require the accurate phase characterization of the field reflected by the single radiating element, to properly choice the dimensions and distributions of the grid radiators giving a radiated field with prescribed features. The reflecting response of microstrip reflectarray elements can be characterized by inserting a periodic array of identical radiators into the open resonator system (Fig. 8). The array grid is chosen to be sufficiently large (typically greater than 5 x 5 elements) in order to better approximate the assumption of infinite array analysis [21].

The grounded reflecting surface can be modelled by the equivalent circuit of Fig. 9, where the relative parameters L_1, C_1 representing the grid depend on the variable length L of the reflectarray patches as well as on the grid spacing between adjacent elements.

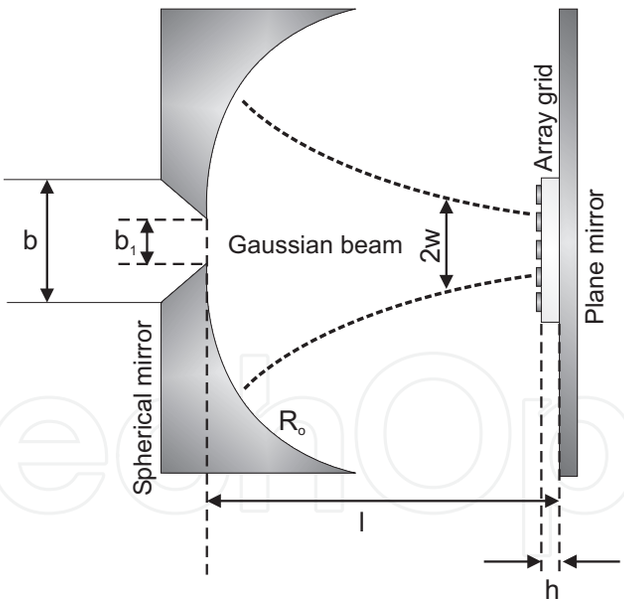

Figure 8. Open resonator system for reflectarray elements characterization

Due to the small thickness h of the usually adopted substrates (typically less than a quarter wavelength), and assuming neglecting losses in the dielectric support, an equivalent inductance L_u can be considered to model the slab, as given by the expression:

$$L_u = Z_d tan\left(k_d h - \phi_G\right) \tag{10}$$

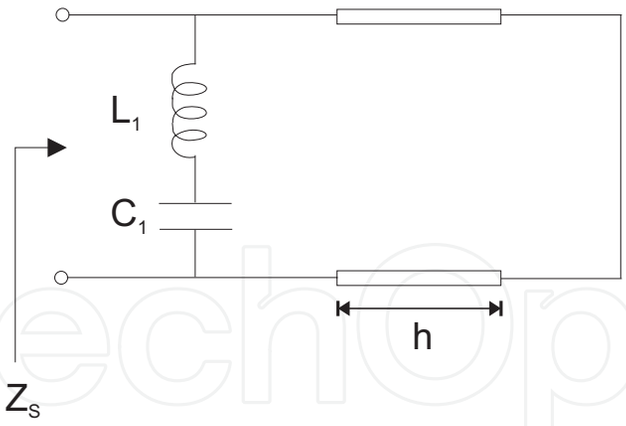

Figure 9. Equivalent circuit relevant to the grounded reflecting grid

where $Z_d = \frac{Z_o}{\sqrt{\epsilon_r}}$, $k_d = k_o\sqrt{\epsilon_r}$, ϵ_r is the relative permittivity of the dielectric and the term ϕ_G is given by eq. (6).

Under the above assumptions, the equivalent circuit of Fig. 9 simplifies as in Fig. 10.

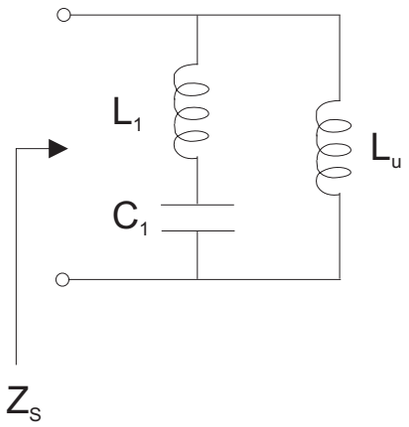

Figure 10. Simplified equivalent circuit relevant to the grounded reflecting grid

Its introduction in the original circuit of Fig. 2 affects the open resonator behavior, which consequently shows two resonant frequencies $f_{1,2}$ relevant to the circuit of Fig. 11.

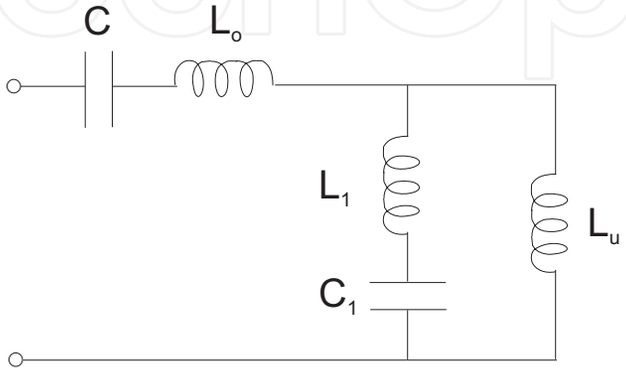

Figure 11. Resonant circuit for the computation of frequencies $f_{1,2}$

They can be easily expressed as:

$$f_{1,2} = \frac{1}{2\pi}\sqrt{\frac{c \pm \sqrt{c^2 - 4d}}{2d}} \tag{11}$$

where:

$$c = L_o C(L_1 + L_u)C_1 + CL_1L_uC_1 \tag{12}$$

$$d = L_o C + (L_1 + L_u)C_1 + L_u C \tag{13}$$

From the above equations, it is straightforward to derive a closed expression for the circuit parameters L_1, C_1, given as:

$$L_1 = \frac{C_1A_1 + B_1}{C_1E_1} \tag{14}$$

$$C_1 = \frac{B_2E_1 - B_1E_2}{A_1E_2 - A_2E_1} \tag{15}$$

where:

$$A_n = (2\pi f_n)^2 L_u - (2\pi f_n)^4 L_u L_o C \tag{16}$$

$$B_n = (2\pi f_n)^2 (L_u + L_o)C - 1 \tag{17}$$

$$E_n = (2\pi f_n)^4 (L_u + L_o)C - (2\pi f_n)^2 \tag{18}$$

for $n = 1, 2$.

The procedure for the reflecting behavior characterization of reflectarray elements can be summarized as follows:

1. insert a sufficiently large array grid of identical square patches having side L and spaced by a distance D;
2. measure the return loss at the waveguide input and derive from it the resonant frequencies $f_{1,2}$ as given by eq. (11);
3. compute the equivalent circuit parameters L_1, C_1 as given by eqs. (14), (15) to have a full characterization of the modelling circuit in Fig. 10 and finally use it to compute the reflection coefficient of the array grid.

The outlined characterization method needs to be obviously repeated for different values of the patch length L in order to retrieve the reflectarray element response as a function of the tuning geometrical parameter.

4.1. K-band phase response characterization of reflectarray elements

The K-band open resonator system of Fig. 4 is adopted to validate the reflectarray elements characterization method outlined in the previous Section. Reflectarray grids composed of 16 x 16 identical square patches with a spacing $D = 0.65\lambda_o$ are considered, for three different values of the patch length L namely L = 3.2 mm, 3.5 mm, 3.7 mm. A dielectric substrate oh thickness h = 0.762 mm and relative permittivity ϵ_r = 2.33 is assumed as support. A

photograph showing the open resonator system loaded with a test reflecting surface is reported in Fig. 12(a), with a particular illustrating the reflectarray grid in Fig. 12(b).

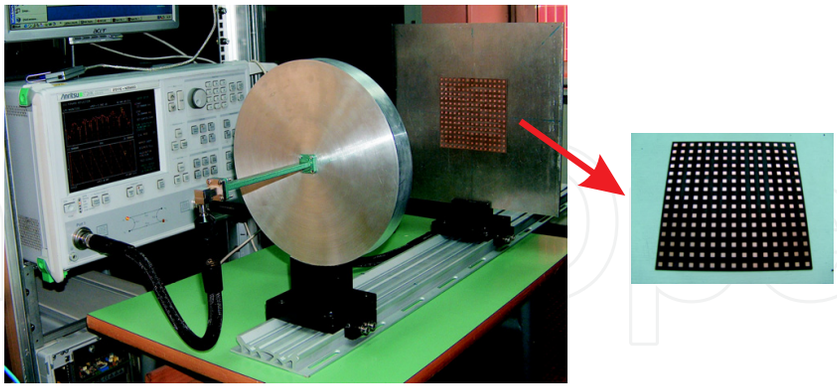

(a) (b)

Figure 12. Photograph of open resonator system (a) loaded with the reflecting surface (b)

To derive the reflectarray element behavior, the return loss magnitude at the waveguide input is measured for the three different values of the patch side L. For all cases, as illustrated in Figs. 13-15, several resonance couples are visible, corresponding to the various modes excited into the cavity. However, the only couple to be considered is that modelled by the equivalent circuit of Fig. 2, corresponding to the $TEM_{0,0,131}$ mode, which is associated to an empty cavity resonance $f_o = 24GHz$.

In the presence of each reflecting surface, two resonant frequencies $f_{1,2}$ are produced, as highlighted in the previous section. They can be easily identified in the return loss measurements (Figs. 13-15) as follows:

i) For a patch side dimension L less than that providing the resonance condition, frequency f_1 is chosen as the nearest one (at the left side) to the resonance frequency f_o of the empty cavity, while the frequency f_2 corresponds to the resonance of the reflectarray grid, easily computed on the basis of the patch dimension L. This is the case corresponding to Fig. 13.

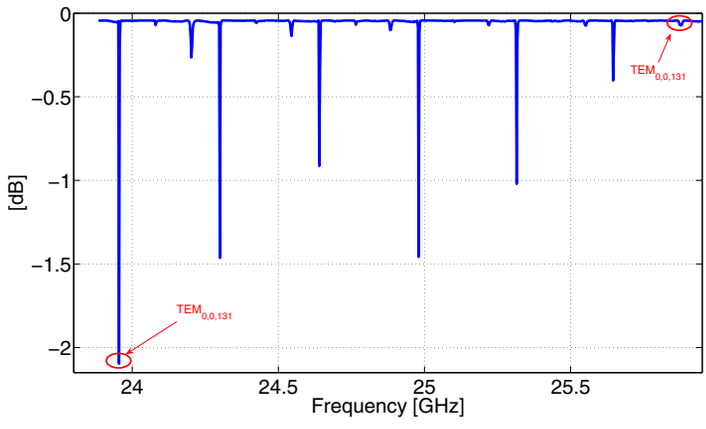

Figure 13. Measured return loss for the case L = 3.2 mm

ii) For a patch side dimension L equal to that providing the resonance condition, frequencies $f_{1,2}$ are chosen as those which are equally far from the resonance frequency f_o of the empty cavity. This is the case corresponding to Fig. 14.

iii) For a patch side dimension L greater than that providing the resonance condition, frequency f_1 is chosen as the nearest one (at the right side) to the resonance frequency f_o of the empty cavity, while the frequency f_2 corresponds to the resonant frequency of the reflectarray grid, again computed on the basis of the patch dimension L. This is the case corresponding to Fig. 15.

The relevant resonances are highlighted in Figs. Figs. 13-15 and summarized in Table 4.

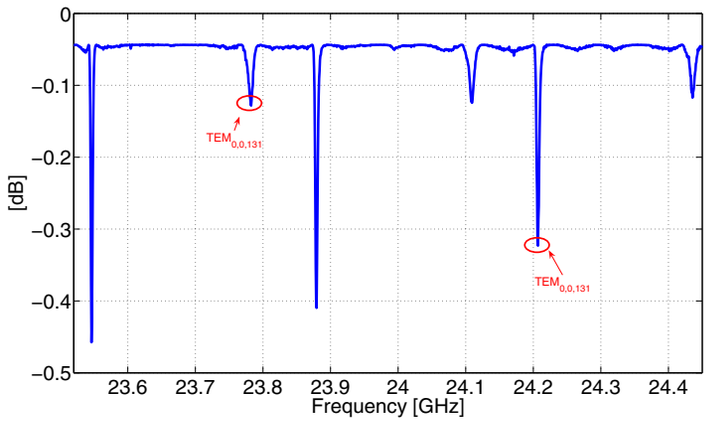

Figure 14. Measured return loss for the case $L = 3.5$ mm

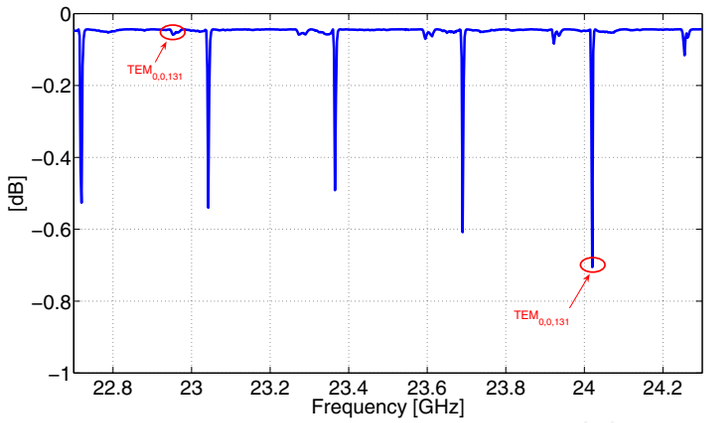

Figure 15. Measured return loss for the case $L = 3.7$ mm

Patch side L [mm]	f_1 [GHz]	f_2 [GHz]	L_1 [nH]	C_1 [fF]
3.2	23.95	25.88	4.06	7.55
3.5	23.78	24.22	4.24	8.44
3.7	22.95	24.02	3.54	8.7

Table 4. Measured resonant frequencies $f_{1,2}$ and relative circuit parameters of Fig. 10

The values of retrieved L_1, C_1 parameters are inserted into the circuit of Fig. 10 to compute the reflection phase relevant to the array grid as a function of frequency. The resulting data are successfully compared in Figs. 16-18 with results coming from Ansoft Designer simulations, for the three different dimensions of patch side L.

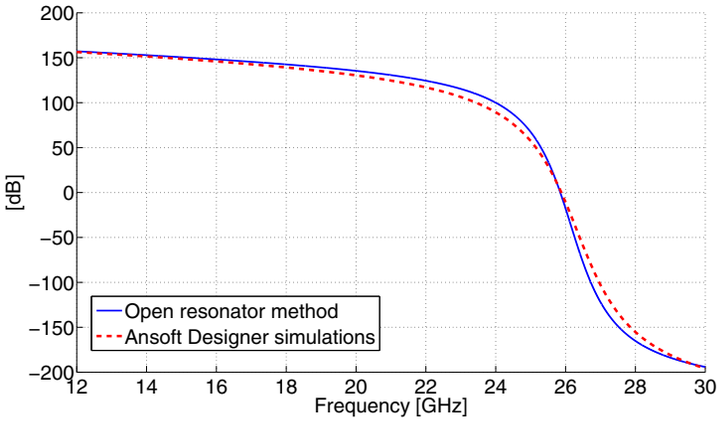

Figure 16. Reflection phase vs. frequency for the case $L = 3.2$ mm

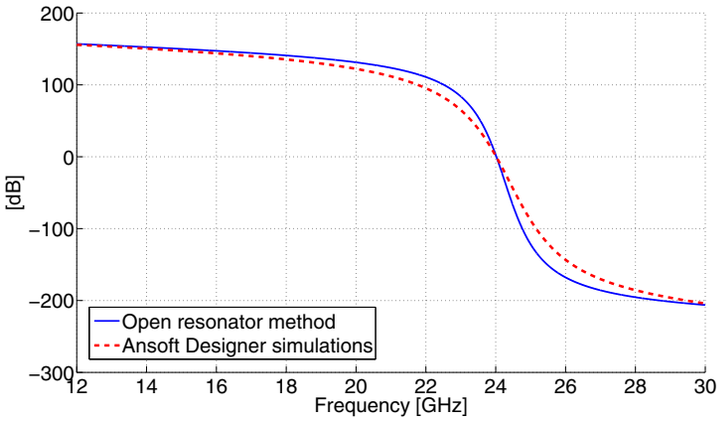

Figure 17. Reflection phase vs. frequency for the case $L = 3.5$ mm

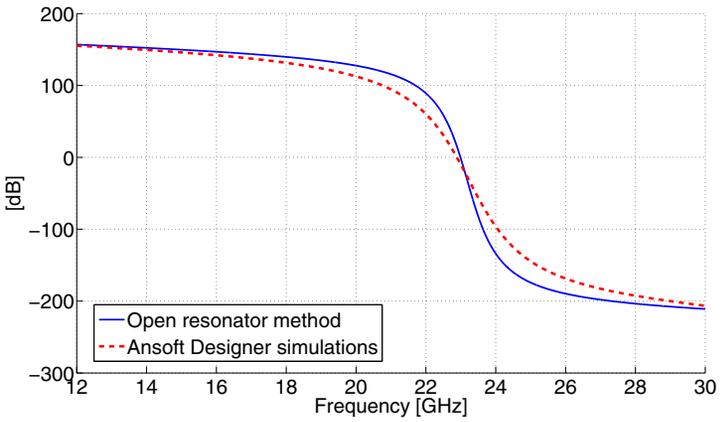

Figure 18. Reflection phase vs. frequency for the case $L = 3.7$ mm

Finally, the parametric results shown in Figs. 16-18 are combined to derive the phase design curve of the reflectarray element as a function of the tuning length L (Fig. 19). Again, a successfull comparison can be observed with Ansoft Designer simulations, thus demonstrating the effectiveness of the proposed approach.

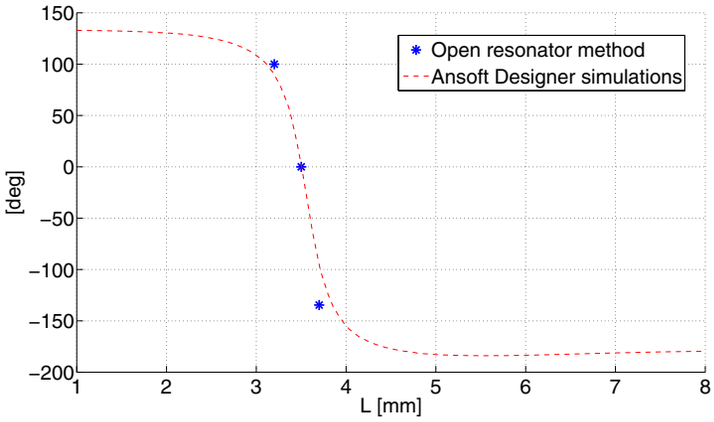

Figure 19. Reflection phase vs. patch side L

5. Conclusion

An equivalent circuit approach has been adopted in this chapter to model an open resonator system used for the equivalent impedance characterization of planar surfaces. On the basis of a full modal analysis, an accurate modelling of the open cavity is performed, taking also into account for the diffraction and the ohmic losses. This approach has led to the optimization of the coupling between the feeding waveguide and the open cavity, thus providing a significant improvement with traditional open resonator methods. The approach has been successfully applied in the framework of two specific application contexts, namely the complex permittivity retrieval of thin dielectric substrates and the phase response characterization of microstrip reflectarrays elements. In both cases, the effectiveness of the method has been experimentally demonstrated by discussing the results obtained from the application of a K-band open resonator system loaded with thin dielectric substrates and small reflectarray grids.

Author details

Sandra Costanzo, Giuseppe Di Massa and Hugo Oswaldo Moreno
University of Calabria, Italy

6. References

[1] Afsar, M. N., Birch, J. R., Clark, R. N. & Chantry, G. W. (1986). The measurement of the properties of materials. *Proc. of IEEE*, Vol. 74, (1986) page numbers (183-199).

[2] Afsar, M. N. & Button, K. J. (1985). Millimeter-wave dielectric measurement of materials. *Proc. of IEEE*, Vol. 73, (1985) page numbers (131-153).

[3] Bialkowski, M. E. & Song, H. J. (1999). Investigations into power-combining efficiency of microstrip patch transmit arrays. *Microwave Opt. Tech. Letters*, Vol. 22, (1999) page numbers (284-287).
[4] Boughriet, A.-H., Legrand, C. & Chapoton, A. (1997). Noniterative stable transmission/reflection method for low-loss material complex permittivity determination. *IEEE Trans. Microwave Theory Tech.*, Vol. 45, (1997) page numbers (52-57).
[5] Bucci, O. M. & Di Massa, G. (1992). Open resonator powered by rectangular waveguide. *IEEE Proc. H*, Vol. 139, (1992) page numbers (323-329).
[6] Costanzo, S., Venneri, I., Di Massa, G. & Borgia, A. (2010). Benzocyclobutene as substrate material for planar millimeter-wave structures: dielectric characterization and application. *Int. Journal of Infrared and Millimeter Waves*, Vol. 31, (2010) page numbers (66-77).
[7] Cullen, A. L. & Yu, P. K. (1979). Complex source-point theory of the elecromagnetic open resonator. *Proc. Royal Soc. Lond. A*, Vol. 366, (1979) page numbers (155-171).
[8] Di Massa, G., Costanzo, S. & Moreno, O. H. (2012). Accurate circuit model of open resonator system for dielectric material characterization. *J. of Electromagn. Waves and Appl.*, Vol. 26, (2012) page numbers (783-794).
[9] Djordjevic, A. R., Biljic, R. M., Likar-Smiljanic V. D. & Sarkar, T. P. (2001). Wideband frequency-domain characterization of FR-4 and time-domain causality. *IEEE Trans. Electrom. Compat.*, Vol. 43, (2001) page numbers (662-667).
[10] Dudorov, S. N., Lioubtchenko, D. V., Mallat, J. A. & Risnen, A. V. (2005). Differential open resonator method for permittivity measurements of thin dielectric film on substrate. *IEEE Trans. Microwave Theory Tech.*, Vol. 54, (2005) page numbers (1916-1920).
[11] Gui, Y. F., Dou, W. B., Su, P. G. & Yin, K. (2009). Improvement of open resonator technique for dielectric measurement at millimetre wavelengths. *IET Microwave Ant. Propag.*, Vol. 3, (2009) page numbers (1036-1043).
[12] Hasar, U. C. & Simsek, O. (2009). An accurate complex permittivity method for thin dielectric materials. *Progress In Electromagnetics Research, PIER*, Vol. 91, (2009) page numbers (123-138).
[13] Hirvonen, T. M., Vainikainen, P., Lozowski, A. & Raisanen, A. V. (1996). Measurement of dielectrics at 100 GHz wit an open resonator connected to a network analyzer. *IEEE Trans. Instrum. Measurements*, Vol. 45, (1996) page numbers (780-786).
[14] Janezic, M. D., Williams, D. F., Blaschke, V., Karamcheti, A. & Chang, C. S. (2003). Permittivity characterization of low-k thin films from transmission-line measurements. *IEEE Trans. Microwave Theory Tech.*, Vol. 51, (2003) page numbers (132-136).
[15] Jones, R. G. (1976). Precise dielectric measurements at 35 GHz using an open microwave resonator. *Proc. IEEE*, Vol. 123, (1976) page numbers (285-290).
[16] Li, K., McLean, S. J., Greegor, R. B., Parazzoli, C. G. & Tanielian, M. H. (2003). Free-space focused-beam characterization of left-handed materials. *Applied Physics Letters*, Vol. 82, (2003) page numbers (2535-2537).
[17] Linch, A. C. (1982). Measurement of permittivity by means of an open resonator. II Experimental. *Proc. Royal Soc. Lond. A*, Vol. 380, (1982) page numbers (73-76).
[18] Marsland, T. P. & Evans, S. (1987). Dielectric measurements with an open-ended coaxial probe. *IEEE Proc. H*, Vol. 134, (1987) page numbers (341-349).

[19] Napoli, L. S. & Hughes, J. J. (1971). A simple technique for the accurate determination of the microwave dielectric constant for microwave integrated circuit substrates. *IEEE Trans. Microwave Theory Tech.*, Vol. 19, (1971) page numbers (664-665).
[20] Olyphant, M. & Ball, J. H. (1970). Strip-line methods for dielectric measurements at microwave frequencies. *IEEE Trans. Electric. Insul.*, Vol. 5, (1970) page numbers (26-32).
[21] Pozar, D. M., Targonski, S. D. & Syrigos, H. D. (1997). Design of millimeter wave microstrip reflectarrays. *IEEE Trans. Antennas Propag.*, Vol. 45, (1997) page numbers (287-296).
[22] Sheen, J. (2005). Study of microwave dielectric properties measurements by various resonant techniques. *Measurement*, Vol. 37, (2005) page numbers (123-130).
[23] Thompson, D. C., Tantot, O., Jallageas, H., Ponchak, G. E., Tentzeris, M. M. & Papapolymeron, J. (2004). Characterization of liquid crystal polymer (LCP) material and transmission lines on LCP substrates from 30 to 110 GHz. *IEEE Trans. Microwave Theory Tech.*, Vol. 52, (2004) page numbers (1343-1352).
[24] Venneri, F., Costanzo, S., Di Massa, G. & Angiulli, G. (2005). An improved synthesis algorithm for reflectarrays design. *IEEE Antennas Wireless Propag. Letters*, Vol. 4, (2005) page numbers (258-261).
[25] Yu, P. K. & Cullen, A. L. (1982). Measurement of permittivity by means of an open resonator. I Theoretical. *Proc. Royal Soc. Lond. A*, Vol. 380, (1982) page numbers (49-71).